

Hydraulic Modeling and
Economic Optimization of
Hollow Fiber Membranes

07442
By
Lt. Eric S. Odderstol, CEC, USN

Prepared for
M. M. Clark
CE 497
University of Illinois

August 2, 1991

120512
02442
C.1

TABLE OF CONTENTS:

Table of Contents.....	i
List of Figures.....	ii
List of Tables.....	iii
Introduction.....	1
The Hydraulic Model.....	3
Solution of the Hydraulic Model.....	10
Results.....	16
Discussion.....	18
Further research.....	19
Economic Optimization.....	28
Discussion/Further research.....	35
Appendix A.....	36
References.....	40

LIST OF FIGURES

1. Laboratory Set up of the UF system.....	4
2. The Hydraulic Model.....	4
3. Moody Diagram.....	7
4. Cross section of the membrane fiber.....	7
5. Comparison of V_f for experiment # 1.....	20
6. Comparison of Q_m for experiment # 1.....	21
7. Comparison of Q_p/Q_m for experiment # 1.....	22
8. Comparison of P_1 for experiment # 1.....	23
9. Comparison of V_f for experiment # 2.....	24
10. Comparison of Q_m for experiment # 2.....	25
11. Comparison of Q_p/Q_m for experiment # 2.....	26
12. Comparison of P_1 for experiment # 2.....	27
13. Pump Curve.....	29
14. Permeate flow as a function of time.....	30
15. Inlet pressure vs. time.....	32
16. Permeate volume per kWH as a function of time.....	34
A-1. Hydraulic Model Spread sheet layout.....	37
A-2. Hydraulic Model Spread sheet output windows.....	38
A-3. Hydraulic Model Spread sheet Input Windows.....	39

LIST OF TABLES

1. Evaluation of friction factor.....	6
2. Evaluation of membrane constant (experiment #'s 1,2).....	10
3. Evaluation of membrane constant (manufacturer's data).....	10
4. Hydraulic model output data (experiment # 1).....	17
5. Hydraulic model output data (experiment # 2).....	17
6. Optimization of V_p per kWH (calculus solution).....	33
7. Optimization of V_p per kWH (graphical solution).....	33

Introduction

An increased interest over the past few years in the use of ultrafiltration processes for the treatment of surface and ground water has prompted a number of studies to evaluate economic advantages of UF over other types of treatment processes. The primary obstacle in making an accurate economic evaluation has been the ability to accurately model the response of the UF process to membrane fouling. We will interest ourselves specifically with hollow fiber membrane modules, and attempt to accurately model UF system parameters with a hydraulic equivalent of the UF system.

Models based on mass transfer (film) theory and the series resistance model have been somewhat effective, but have had specific limitations in their application (Cheryan 1986, Clark 1991, Lainé 1989). The mass transfer model presented by Cheryan (pp.84-89) assumes system operation in a region where permeate flux is independent of system pressure. In this model, the permeate flux is described in terms of boundary layer concentration, gel layer concentration, and mass transfer coefficient; although possible to derive a solution based on these parameters, the solution technique is somewhat cumbersome and does not relate permeate flow to other system parameters, nor does it allow for a solution when the system is operating within the pressure controlled region. Because the hollow fiber membrane typically operates at such pressures, we will not pursue further investigation of the mass transfer model. The series resistance model discussed by Clark and Lainé has the advantage of effectively modeling system response in the pressure controlled region, but does not allow for the possible interdependence of the various resistance terms (Lainé, 1989, p.66), nor does it allow for non-linear relationships between flow and pressure within the system (Clark, 1991, p.14).

The motivation for this report was a suggestion by Clark (1991) that simple membrane fouling models could be incorporated in an overall UF system hydraulic model. The hydraulic model we will develop will differ from the models described above in that we will attempt to describe the UF system as a whole as opposed to modeling only the membrane permeate flux. As we shall see, this approach will allow for a relatively simple economic analysis of UF pilot system operations. The hydraulic model will also offer the advantages of allowing for the interdependence of the various head loss terms and for the non-linearity of head loss as a function of operating pressure and flow rate. The model further allows the user to input any number of membrane fouling schemes directly into the model by varying a single parameter.

The hydraulic model developed here is based on the application of fundamentals of fluid mechanics to the UF pilot system. The head loss through the membrane fibers as well as the head loss of the permeate passing through the membrane are developed such that they can be expressed in terms of easily measured system operating parameters. Head loss terms for system valves and pipes are

developed in the same manner. A physical property of the membrane, referred to as the membrane constant, is introduced, referring to the inherent resistance of the membrane to permeate flow. Although a physical constant of the membrane, it may be regarded as a property of the membrane which one can vary with either time or permeate volume, thus allowing for the modeling of system response to various membrane fouling scenarios.

Once the model has been solved, the data output may be used to determine an optimal operating period for the ultrafiltration and back flush cycles. This economic optimization will determine the cycle time for which permeate flow per kilowatt hour of energy consumed is maximized.

The Hydraulic Model

Figure (1) shows the laboratory set up of the ultrafiltration system to be modeled. Figure (2) is the hydraulic equivalent of the system. For analysis purposes, we shall consider a closed system where both permeate and retentate are returned to the pump suction. We shall describe each component of the system in terms of flow and head loss, write the associated head loss equations, and then develop a solution procedure for several scenarios.

System Components:

Pump head: The head delivered by the pump is described by the pump curve. Although the pump curve is different for each pump, it can generally be described by the following equation:

$$\Delta P_p = A Q_t^2 + B Q_t + C \quad (1)$$

where ΔP is the pump discharge pressure, Q_t is the flow generated by the pump, and the constants A, B, and C are the results of a "least squares" fit of the pump curve (for the pump used in this model, $A=-36.943$, $B=61.66335$, and $C=63.40662$) (Clark, 1991).

Height differential head loss: The model as constructed in the lab had a short height differential between the pump and the inlet to the membrane. The head loss associated with the change in height is given by

$$\Delta P_z = \rho g z \quad (2)$$

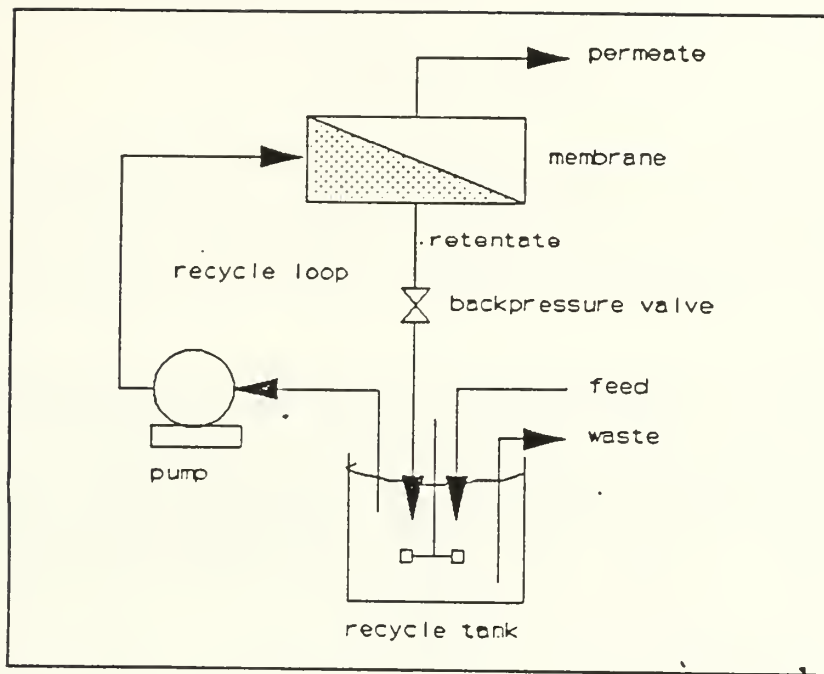
where ρ is the fluid density (kg/m^3), g is the acceleration due to gravity, h_f is the head loss due to the height differential, and z is the height differential.

System tubing head loss: Head loss in the system tubing is described by the Darcy-Weisbach Equation:

$$h_f = \frac{f L V^2}{2 g d} \quad (3)$$

where L is the length of the tube, f is the friction factor, V is the velocity of the fluid through the tube, and d is the tube diameter. Substituting $\Delta P_t = \rho g h_f$ into equation (3), we get

$$\Delta P_t = \frac{\rho f L V^2}{2 d} \quad (4)$$



Source: Clark, 1991

Figure (1)

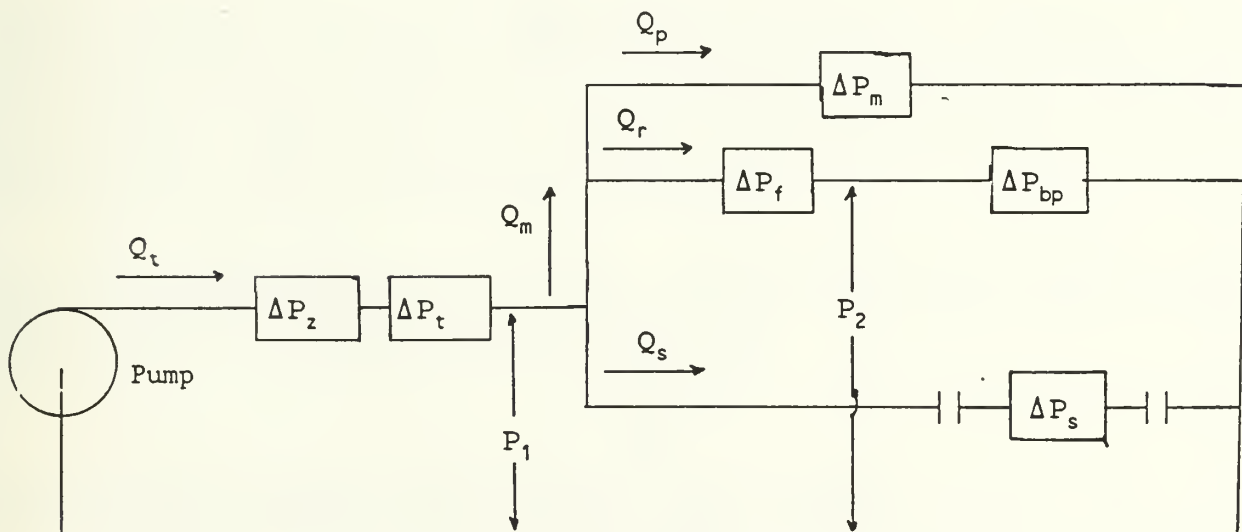


Figure (2)

The flow through the system tubing is turbulent ($Re \approx 4000$) and the friction factor, f , can be determined through use of the Moody diagram. For the analytical approach we will use in solving the hydraulic model, the Moody diagram can be approximated by the following equation (White, p. 313-314):

$$f \approx \left\{ -1.8 \log \left[\left(\frac{6.9}{Re} \right) + \left(\frac{\epsilon}{3.7d} \right)^{1.11} \right] \right\}^{-2} \quad (5)$$

where ϵ is the tube roughness. We shall assume a fairly "smooth" tube, with a roughness of .0015 mm. We shall further assume, for purposes of this analysis, that the length of the tube from the permeate exit to the pump suction is zero; this assumption reflects the laboratory condition of the permeate discharging directly into a separate container.

Valve head loss: There are two valves in the piping network; one which provides back pressure to the fiber module, and one which provides for a bypass of the fiber module. The latter is included in the system to allow for the use of pumps of varying size in the system. If the pump is properly sized for the membrane in use, the bypass line is not required. The head loss for each valve is described by the following equation:

$$h_f = \frac{KV^2}{2g} \quad (6)$$

Substituting $\Delta P = \rho gh_f$ into equation (6), we get

$$\Delta P = \frac{\rho KV^2}{2} \quad (7)$$

In each equation, K represents a proportionality constant which, unfortunately, cannot be expressed in terms of roughness and Reynold's Number (White, p.333). Values of K are listed in most Fluid Mechanics references for valves of various designs and sizes. The valves we used were not listed in these references, and had to be measured experimentally by measuring the flow rate and the associated pressure drop across the valve.

Fiber Head loss: A 'typical' fiber is shown in figure (4). The flow through each fiber of the membrane is in the transitional region between laminar and turbulent flow. The head loss is again described by the Darcy-Weisbach equation:

$$h_f = \frac{f L_f V_f^2}{2g d_f} \quad (8)$$

Substituting $\Delta P_f = \rho gh_f$ into equation (8), we get

$$\Delta P_f = \frac{\rho f L_f V_f^2}{2 d_f} \quad (9)$$

For laminar flow, the friction factor is given by the expression

$f = 64/R_e$. For turbulent flow, the friction factor is given by equation (5). Again, we are limited by not knowing the roughness of the membrane fiber. We can, however, solve for roughness using experimental results. By obtaining measurements of membrane flow, we can calculate fiber velocity with the equation

$$V_f = \left(\frac{Q_m + Q_r}{2n} \right) \left(\frac{1}{a_f} \right) \quad (10)$$

which is simply the average flow through one fiber divided by the cross sectional area of that fiber; n is the number of fibers in the membrane cartridge (the membrane we used had $n = 20$ fibers), Q_m is the inlet flow to the membrane, Q_r is the retentate flow rate, and a_f is the cross sectional area of a single fiber. Once fiber velocity is known, we can use equation (9) to solve for the friction factor:

$$f = \frac{2 d_f \Delta P_f}{\rho L_f V_f^2} \quad (11)$$

Now having both the friction factor and the fiber velocity, we can solve for ϵ in equation (5). The results of these calculations for two different experiments are shown in table (1), giving an average ϵ of 7.64×10^{-5} meters.

TABLE (1)
EVALUATION OF FRICTION FACTOR FROM VARIOUS DATA:

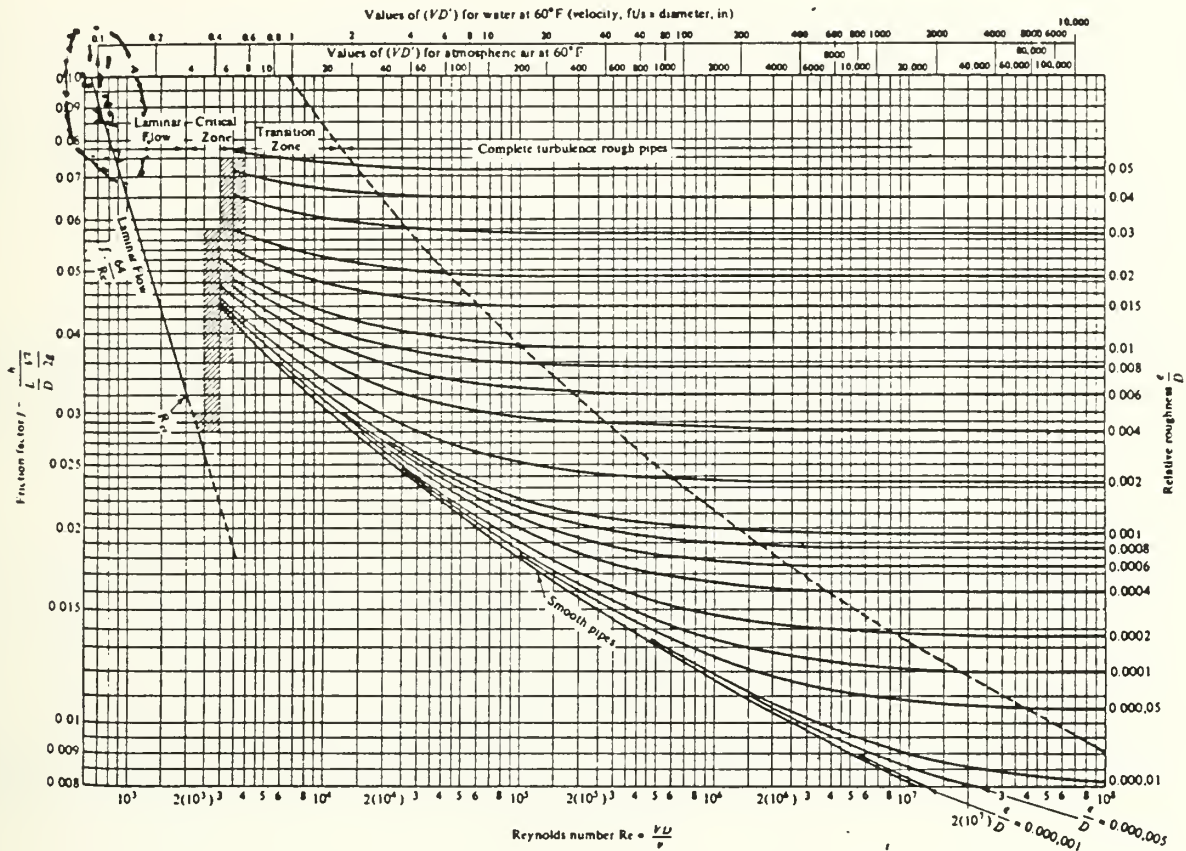
CONSTANTS:							
	ρ	d_f	μ	L_f			
	(kg/m ^{^3})	(m)	(kg/m-sec)	(m)			
	997.4	0.00093	9.42E-04	1.03			
<u>EXPERIMENT # 1:</u>							
Q_m	Q_p	Q_r	V_f	ΔP_f	R_e	f	ϵ
(l/min)	(l/min)	(l/min)	(m/sec)	(N/m ²)			(m)
1.547	0.387	1.160	0.949	57918.0	934.39	0.117	9.09E-05
1.621	0.381	1.240	0.994	66881.5	978.97	0.123	1.03E-04
1.562	0.402	1.160	0.958	59297.0	943.39	0.117	9.21E-05
1.573	0.393	1.180	0.965	60676.0	950.03	0.118	9.42E-05
AVG:							9.51E-05

Source: Heneghan, 1991

EXPERIMENT # 2:							
Q_m	Q_p	Q_r	V_f	ΔP_f	R_e	f	ϵ
(l/min)	(l/min)	(l/min)	(m/sec)	(N/m ²)			(m)
0.785	0.145	0.640	0.874	36791.7	860.87	0.087	3.57E-05
1.163	0.213	0.950	1.296	68484.6	1276.80	0.074	2.47E-05
0.973	0.179	0.795	1.085	56587.3	1068.18	0.087	4.22E-05
0.637	0.126	0.511	0.704	34492.2	693.22	0.126	9.93E-05
0.963	0.153	0.811	1.088	56487.3	1071.60	0.086	4.11E-05
0.798	0.149	0.649	0.888	46289.6	874.56	0.106	7.04E-05
0.768	0.288	0.480	0.766	39791.0	754.34	0.123	9.61E-05
0.818	0.078	0.740	0.956	47882.3	941.52	0.095	5.21E-05
AVG:							5.77E-05

Source: Adham, 1991

The Moody Diagram is a plot of f vs. Re for various ϵ/d ratios (figure (3)). Note that the data plotted for the two experiments lie in the transition region between laminar and turbulent flows, though each experiment tends lie closer to the laminar flow region.



Source: White, p. 313.

Figure (3)

Permeate flow head loss: Permeate flow through each membrane pore is considered to be laminar flow because of low Reynold's numbers (<1800) obtained from experimental data for various membranes (Cheryan, p.76-77). Figure (4) shows a side view of a 'typical' fiber.

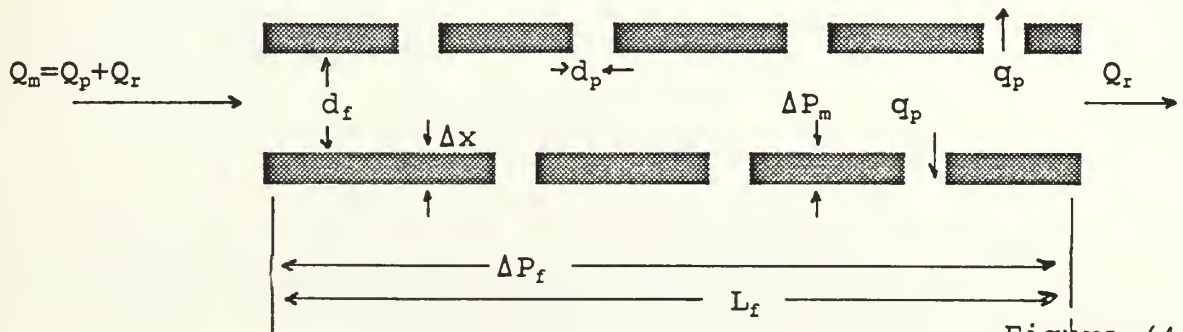


Figure (4)

In general terms, the head loss through a single pore is given by the Darcy-Weisbach equation:

$$h_f = \frac{f \Delta x V_p^2}{2g d_p} \quad (12)$$

where f is the friction factor, Δx is the membrane "skin" thickness, V_p is the velocity of the fluid through the pore, g is the acceleration due to gravity, and d_p is the diameter of the pore. For laminar flow, the friction factor is given by $f = 64/R_e$. Substituting into equation (12) gives

$$h_f = \frac{32 \mu \Delta x V_p}{\rho g d_p^2} \quad (13)$$

Our goal is to express the permeate head loss in experimentally measurable terms. To do so, we will express equation (13) in terms of pore flow rate, pore area, and pore radius:

$$V_p = \frac{Q_p}{A_p} \quad d_p = 2r_p \quad (14)$$

Substituting equation (14) into equation (13), we get

$$h_f = \frac{8 \mu \Delta x q_p}{\rho g a_p r_p^2} \quad (15)$$

We shall assume that the membrane in question has a total of "n" pores. The total flow through the membrane, then, is given by

$$Q_p = \sum_{i=1}^n q_{p_i} \quad (16)$$

The surface porosity of the membrane is defined as the ratio of total pore area to total membrane surface area. If porosity and surface area (A) are known, then the total pore area may found:

$$A_p = \sum_{i=1}^n a_{p_i} = \epsilon A \quad (17)$$

We now substitute equations (16) and (17) into equation (14) to describe the total flow through the membrane:

$$V_p = \sum_{i=1}^n \left(\frac{q_{p_i}}{a_{p_i}} \right) = \frac{Q_p}{\epsilon A} \quad (18)$$

These expressions may now be used to express h_f in terms of the membrane area, porosity, and total permeate flow:

$$h_f = \frac{8 \mu \Delta x Q_p}{\rho g r_p^2 \epsilon A} = \frac{8 \mu \Delta x q_p}{\rho g a_p r_p^2} \quad (19)$$

The permeate head loss across the membrane surface may be expressed in terms of a change in pressure across the membrane. Because the pressure drops along the length of the membrane fiber (due to fiber head loss), we will use the average pressure drop across the membrane, hereafter referred to as the "trans-membrane" pressure:

$$\Delta P_m = \frac{P_1 + P_2}{2} \quad (20)$$

where P_1 is the membrane cartridge inlet pressure, and P_2 is the outlet pressure. The relationship between pressure and head loss is given by

$$\Delta P_m = \rho g h_f \quad (21)$$

Substituting into equation (19), we obtain

$$\Delta P_m = \frac{8\mu \Delta x Q_p}{r_p^2 e A} \quad (22)$$

The limitation of equation (22) is that membrane thickness, porosity, and pore radius are generally not known. These terms, however, do represent a physical constant of the clean membrane. If trans-membrane pressure and permeate flow can be measured experimentally, we can reasonably estimate the unknown parameters. We shall then define the membrane constant, C , as

$$C = \frac{\Delta x}{e r_p^2} \quad (23)$$

with units of $1/L$. Equation (22) then becomes

$$\Delta P_m = \frac{8\mu C Q_p}{A} \quad (24)$$

Table (2) shows the calculation of the membrane constant for the same membrane using data from two different experiments (Heneghan, 1991, Adham, 1991)[†]. The results compare favorably with each other, as well as with values obtained for various membranes from manufacturer's data (Table (3)).

[†] The membrane used in these experiments was BCDA cellulose acetate, with a Molecular Weight cutoff around 100k daltons, manufactured by Yonaïse des Eaux, Paris, France.

TABLE 2

EVALUATION OF MEMBRANE CONSTANT

EXPERIMENT # 1:

TEST #	ΔP_t	Q_p	Q_p	C
	(N/M ²)	(l/min)	(M ³ /sec)	1/M
1	1.307E+05	0.3978	6.630E-06	1.569E+11
2	1.517E+05	0.3867	6.445E-06	1.874E+11
3	1.527E+05	0.3805	6.342E-06	1.918E+11
4	1.531E+05	0.4016	6.693E-06	1.821E+11
5	1.565E+05	0.3926	6.543E-06	1.905E+11
AVG:	1.489E+05	0.39184	6.531E-06	1.880E+11

EXPERIMENT # 2:

TEST #	ΔP_t	Q_p	Q_p	C
	(N/M ²)	(l/min)	(M ³ /sec)	1/M
1	6.647E+04	0.1450	2.4167E-06	2.112E+11
2	9.901E+04	0.2132	3.5528E-06	2.141E+11
3	8.115E+04	0.1785	2.975E-06	2.095E+11
4	5.316E+04	0.1258	2.0972E-06	1.947E+11
5	6.757E+04	0.1528	2.5472E-06	2.037E+11
6	6.481E+04	0.1490	2.4833E-06	2.005E+11
7	1.350E+05	0.2880	4.8E-06	2.160E+11
8	3.199E+04	0.0782	1.3028E-06	1.886E+11
AVG:	7.490E+04	0.1663	2.772E-06	2.048E+11

AVERAGE OF THE TWO: 1.964E+11

TABLE 3

EVALUATION OF MEMBRANE CONSTANTS FROM MANUFACTURER'S DATA:

d	r	AREA	PORE DENSITY	POROSITY	Δx	C
(μ m)	(μ m)	(μ m ²)	(PORES/cm ²)		(μ m)	
0.9	0.45	0.63617251	20000000	0.1272345	11.5	4.463E+08
0.18	0.09	0.0254469	300000000	0.0763407	12	1.941E+10
0.09	0.045	0.00636173	300000000	0.01908518	5.3	1.371E+11
0.072	0.036	0.0040715	300000000	0.01221451	5.4	3.411E+11
0.045	0.0225	0.00159043	600000000	0.00954259	5.4	1.118E+12
0.027	0.0135	0.00057256	600000000	0.00343533	5.4	8.625E+12

Source: Cheryan, 1986, p.60

Solution of the Hydraulic Model:

We now have all elements of the hydraulic model described in terms of pressure drop and flow rate, specifically the head loss terms for the pump, height differential, system tubing, system valves, the membrane fibers, and the membrane pores (equations 1,2,4,7,9, & 24). All that is left to do is solve for the unknown pressures and flow rates. We shall examine four scenarios: Laminar and turbulent flow solutions without use of a bypass line, and

laminar and turbulent flow solutions for the case when the bypass line is used. Each scenario has been solved using an iterative technique along with a "QUATTRO PRO" spreadsheet program. We shall write the equations here, develop the iterative solution approach, and then show the results obtained through use of the spreadsheet. Note that all pressures are measured in PSIG, lengths in meters, areas in meters squared, and all flow rates are measured in liters per minute. Appropriate conversion factors are indicated.

Case #1: Laminar flow, no bypass valve.

Figure (2) shows the hydraulic model to be solved. The unknowns to be solved for are the membrane cartridge inlet pressure P_1 , Q_t , Q_r , and Q_p . We need, then, four equations to solve for the four unknowns.

The first unknown to solve for is P_1 , the inlet pressure to the membrane. P_1 may be found by subtracting both the inlet tubing head loss and the height differential head loss from the pump head generated by the pump:

$$\begin{aligned} P_1 &= A Q_t^2 + B Q_t + C - \Delta P_z - \Delta P_t, \quad \text{where} \\ \Delta P_z &= \rho g z \\ \Delta P_t &= \frac{\rho f_t L_t Q_t^2}{2 d_t a_t^2} \end{aligned} \quad (25)$$

The second unknown, permeate flow (Q_p) may be found by substituting equation (24) into equation (20):

$$\Delta P_m = \frac{P_1 + P_2}{2} = \frac{8 \mu C Q_p}{A} \quad (26)$$

P_2 is simply the change in pressure across the back pressure valve:

$$P_2 = \Delta P_{bp} = \frac{\rho K_{bp} Q_r^2}{2 a_{bp}^2} \quad (27)$$

Note that we have substituted $V_r = Q_r / a_{bp}$, where a_{bp} is the cross sectional area of the back pressure valve. This substitution will make the ensuing calculations somewhat simpler. Retentate flow, Q_r , is used because only retentate fluid flows through the back pressure valve. We now solve equation (26) for P_1 , and substitute equation (27) for P_2 :

$$P_1 = 2 \left(\frac{8 \mu C Q_p}{A} \right) - \frac{\rho K_{bp} Q_r^2}{2 a_{bp}^2} \quad (28)$$

We shall now introduce constants Z and Y:

$$\begin{aligned} Z &= \left(\frac{8 C \mu}{A} \right) \left(\frac{1}{6895} \right) \left(\frac{1}{60000} \right) \\ Y &= \left(\frac{\rho K_{bp}}{2 A_{bp}^2} \right) \left(\frac{1}{6895} \right) \left(\frac{1}{60000^2} \right) \end{aligned} \quad (29)$$

where the term $(1/6895)$ is a conversion factor from newtons per meter squared to PSI and the term $(1/60000)$ is a conversion factor from cubic meters per second to liters per minute. Substituting Z and Y into equation (28), we get

$$P_1 = 2 Z Q_p - Y Q_r^2 \quad (30)$$

The third unknown, retentate flow, may also be described in terms of P_1 :

$$P_1 = \Delta P_f + \Delta P_{bp} \quad (31)$$

substituting equations (9) and (27), and making the substitution for the constant Y as before, we get

$$P_1 = \left(\frac{64}{R_e} \right) \left(\frac{\rho L_f V_f^2}{2 d_f} \right) + Y Q_r^2 \quad (32)$$

We now substitute $R_e = \rho v d / \mu$:

$$P_1 = \left(\frac{64 \mu}{\rho V_f d_f} \right) \left(\frac{\rho L_f V_f^2}{2 d_f} \right) + Y Q_r^2 \quad (33)$$

Substituting flow rate for velocity using equation (10) (recall $n=20$) gives

$$P_1 = \left(\frac{.8 \mu L_f}{d_f^2 a_f} \right) (Q_t + Q_r) + Y Q_r^2 \quad (34)$$

Note that in the case of no bypass valve, membrane flow Q_m is exactly equal to total flow Q_t . Defining a constant X:

$$X = \left(\frac{.8 \mu L_f}{d_f^2 a_f} \right) \left(\frac{1}{6895} \right) \left(\frac{1}{60000} \right) \quad (35)$$

yields the final form of the equation for P_1 :

$$P_1 = X(Q_t + Q_r) + Y Q_r^2 \quad (36)$$

Finally, we use the continuity equation to solve for the fourth unknown, Q_t :

$$Q_t = Q_p + Q_r \quad (37)$$

The four unknowns are now solved with equations (25,30,36,& 37) in the following manner: First, guess a value for Q_t , and generate a value of change in pressure using equation (25). Then, solve equations (30) and (36) for the quantity $Y \cdot Q_r^2$. To do this, set equations (30) and (36) equal to each other, and substitute $Q_p = Q_t - Q_r$ in equation (30). We arrive, then, at the following solution for Q_r :

$$Q_r = \frac{2 P_1 - Q_t (X + 2 Z)}{X - 2 Z} \quad (38)$$

We can now solve equation (38) based on the results of the assumed value of Q_t . We then use the continuity equation (equation (37) to solve for Q_p :

$$Q_p = Q_t - Q_r \quad (39)$$

We check our estimate of Q_t by solving for change in pressure in equation (30), and iterate on Q_t until the values of P_1 given by equations (25) and (30) match. These calculations are done on the QUATTRO PRO spreadsheet.

Case # 2: No bypass valve, Turbulent flow through membrane fibers.

Because the flow through the membrane fibers is now to be evaluated as turbulent, the equation for the head loss through the membrane fibers is given by

$$P_1 = f \left(\frac{\rho L_f V_f^2}{2 d_f} \right) + Y Q_r^2 \quad (40)$$

where the friction factor f is

$$f \approx \left\{ -1.8 \log \left[\left(\frac{6.9}{Re} \right) + \left(\frac{e}{3.7 d} \right)^{1.11} \right] \right\}^{-2} \quad (41)$$

We now define the constant W :

$$W = \frac{1}{2} \left(\frac{\rho L_f}{d_f} \right) \left(\frac{1}{6895} \right) \quad (42)$$

Substituting into equation (40), we get

$$P_1 = W f V_f^2 + Y Q_r^2 \quad (43)$$

where

$$V_f = \left(\frac{Q_t + Q_r}{40 a_f} \right) \left(\frac{1}{60000} \right) \quad (44)$$

To solve the problem, we first substitute $Q_p = Q_t - Q_r$ into equation (30), and solve for Q_r . The resulting equation is

$$Q_r = \frac{\left(\frac{-2Z}{Y}\right) \pm \sqrt{\left(\frac{2Z}{Y}\right)^2 + 4\left(\frac{2ZQ_p - \Delta P}{Y}\right)}}{2} \quad (45)$$

Once again, we guess a value of Q_t and solve for change in pressure in equation (25). Plugging the results into equation (45) will give two possible values of Q_r , only one of which is feasible (the other will give a negative value). We then solve equation (43) for change in pressure to check our original guess, and then iterate until the two values match. Once again, the calculations are done on the spreadsheet program.

Case # 3: Bypass valve in place, laminar flow solution.

The solution technique for this case is similar to that of case number one; in fact, equations (25) & (30) still apply. Equation (36) remains the same, with one exception: total flow leaving the pump is now split between the bypass valve and the membrane cartridge. The continuity equation now becomes

$$Q_t = Q_s + Q_m, \text{ where } Q_m = Q_p + Q_r \quad (46)$$

Equation (36) now becomes

$$P_1 = X(Q_m + Q_r) + YQ_r^2 \quad (47)$$

The addition of the bypass valve adds a fifth unknown to the problem, the bypass flow (Q_s). This flow can also be expressed as a function of change in pressure and the head loss due to the bypass tubing and the bypass valve:

$$P_1 = f_s \left(\frac{\rho L_s V_s^2}{2 d_s} \right) + \frac{\rho K_s V_s^2}{2} \quad (48)$$

Substituting $V_s = Q_s / a_s$,

$$P_1 = f_s \left(\frac{\rho L_s Q_s^2}{2 d_s a_s^2} \right) + \frac{\rho K_s Q_s^2}{2 a_s^2} \quad (49)$$

We now introduce constants F & G:

$$F = \left(\frac{\rho K_s}{2 a_s^2} \right) \left(\frac{1}{60000^2} \right) \left(\frac{1}{6895} \right) \quad (50)$$

$$G = \left(\frac{\rho L_s}{2 d_s a_s^2} \right) \left(\frac{1}{60000^2} \right) \left(\frac{1}{6895} \right) \quad (51)$$

Substituting equations (50) and (51) into equation (49) yields

$$P_1 = Q_s^2 (F + f_s G) \quad (52)$$

To solve the equations, we again guess a value of Q_t and find the resulting change in pressure by equation (25). The problem now becomes a bit tricky because we can no longer isolate a single flow and solve for it explicitly, even if we were to use a quadratic as before. We can get around this problem by assuming that the factor $f_s * G$ is very small. Then, we can solve for Q_s by

$$Q_s = \sqrt{\frac{P_1}{F}} \quad (53)$$

We can now get Q_m from equation (46), and solve the quadratic of equation (47) for Q_r :

$$Q_r = \frac{-X \pm \sqrt{X^2 - 4Y(XQ_m - \Delta P)}}{2Y} \quad (54)$$

Once Q_r is known, Q_p can be solved for. We check our assumption of Q_t by solving for change in pressure in equation (30), iterating on Q_t until the two values of change in pressure are equal. Again, these calculations are done for us on the spreadsheet.

Finally, we check our assumption that the quantity $f_s * G$ is negligible by solving for change in pressure in equation (52), and comparing with our answer. By doing so, we find that the assumption was reasonable (solution error < 2%). If, however, we want to "fine-tune" the answer, we can now calculate the factor $f_s * G$, plug it into equation (52), and solve the remaining equations as before. As it turns out, the factor $f_s * G$ does not vary much with changing Q_s over the range of values in which we are interested; we can therefore assume a constant value based on a single calculation, giving an improved (though still slightly inaccurate) estimation of Q_s . My calculations gave a value of $f_s * G = .03$. Equation (53) then becomes

$$Q_s = \sqrt{\frac{P_1}{F + .03}} \quad (55)$$

Case # 4: Bypass valve in place, turbulent flow.

For this problem, all equations of case # 3 remain the same, with the exception of equation (47), which must now be replaced by an expression for turbulent flow losses. The method is the same as

was used in case number two; in fact, the equations are the same:

$$P_1 = WfV_f^2 + YQ_f^2 \quad (56)$$

$$V_f = \left(\frac{Q_m + Q_r}{40 a_f} \right) \left(\frac{1}{60000} \right) \quad (57)$$

We solve for change in pressure and Q_s using equations (25) & (55), and for Q_m using equation (46). Using $Q_p = Q_m - Q_r$, we substitute into equation (30) and get

$$P_1 = 2Z(Q_m - Q_r) - YQ_r^2 \quad (58)$$

Solving the quadratic, we obtain

$$Q_r = \frac{-2Z \pm \sqrt{4Z^2 + 4Y(2ZQ_m - \Delta P)}}{2Y} \quad (59)$$

and solve for Q_r . We can then obtain Q_p and check our estimation of Q_t by solving for P_1 in equation (30), again iterating until the values match.

Results: Attempts to simulate the membrane flow characteristics obtained in the lab with the hydraulic model were hampered because of a lack of information concerning the pumps used in lab experiments. Without knowledge of the pump curve for the pump used, an exact comparison of data could not be made. This obstacle was partially overcome by deriving a pump curve equation from known data for a pump which was not used in the experiments. The hydraulic model was then solved, and the resulting bypass flow adjusted until the membrane cartridge influent flow of the hydraulic model matched that of the experiment. The bypass flow for the model was controlled by varying the K value of the bypass valve. Once this match was achieved, a comparison of such parameters as trans-membrane pressure, ratio of permeate to membrane flow, and fibre flow velocity could be made.

Table (4) and table (5) show a comparison of experimental and simulated membrane parameters for two different experiments. Each parameter is also plotted, as shown in figures (5-12). The model responds favorably in most cases; Experiment number two shows results which vary considerably in cases for which inlet pressures which differ from the norm. I would speculate that the discrepancy lies in the possibility that the bypass flow was altered during the time that these data were collected.

TABLE 4
EVALUATE BOTH MODELS FOR EXPERIMENT #1:

TEST CONDITIONS								
TEST #:	C	V _f	Q _p	Q _r	Q _t	Q _m	Q _p /Q _m	P ₁
1	1.57E+11	1.74	0.398	1.22	1.618	1.618	0.246	20.6
2	1.87E+11	1.66	0.387	1.16	1.547	1.547	0.250	26.2
3	1.92E+11	1.75	0.381	1.24	1.621	1.621	0.235	27
4	1.82E+11	1.67	0.402	1.16	1.562	1.562	0.257	26.5
5	1.9E+11	1.69	0.393	1.18	1.573	1.573	0.250	27.1
AVG:	1.82E+11	1.70	0.392	1.19	1.584	1.584	0.247	25.48

LAMINAR FLOW MODEL								
TEST #:	C	V _f	Q _p	Q _r	Q _t	Q _m	Q _p /Q _m	P ₁
1	1.57E+11	1.680	0.428	1.155	2.152	1.584	0.271	24.07
2	1.87E+11	1.684	0.376	1.185	2.142	1.561	0.241	25.11
3	1.92E+11	1.685	0.369	1.189	2.140	1.558	0.237	25.26
4	1.82E+11	1.684	0.384	1.180	2.143	1.564	0.246	24.97
5	1.9E+11	1.684	0.372	1.187	2.141	1.559	0.239	25.20
AVG:	1.82E+11	1.684	0.384	1.180	2.143	1.564	0.246	24.96

TURBULENT FLOW MODEL								
TEST #:	C	V _f	Q _p	Q _r	Q _t	Q _m	Q _p /Q _m	P ₁
1	1.57E+11	1.490	0.451	0.989	2.082	1.440	0.313	30.75
2	1.87E+11	1.497	0.396	1.022	2.071	1.418	0.279	31.78
3	1.92E+11	1.498	0.388	1.027	2.070	1.415	0.274	31.93
4	1.82E+11	1.496	0.404	1.017	2.073	1.421	0.284	31.63
5	1.9E+11	1.497	0.391	1.025	2.070	1.416	0.276	31.87
AVG:	1.82E+11	1.496	0.404	1.017	2.073	1.421	0.284	31.63

TABLE 5
EVALUATE BOTH MODELS FOR EXPERIMENT # 2:

TEST CONDITIONS								
TEST #:	C	V _f	Q _p	Q _r	Q _t	Q _m	Q _p /Q _m	P ₁
1	1.89E+11	0.874	0.145	0.640	0.785	0.785	0.185	9.64
2	1.95E+11	1.296	0.213	0.950	1.163	1.163	0.183	14.36
3	2.00E+11	1.085	0.179	0.795	0.973	0.973	0.183	11.77
4	2.04E+11	0.704	0.126	0.511	0.637	0.637	0.198	7.71
5	2.10E+11	1.088	0.153	0.811	0.963	0.963	0.159	9.80
6	2.11E+11	0.888	0.149	0.649	0.798	0.798	0.187	9.40
7	2.14E+11	0.766	0.288	0.480	0.768	0.768	0.375	19.58
8	2.16E+11	0.956	0.078	0.740	0.818	0.818	0.096	4.64
AVG:	2.05E+11	0.957	0.166	0.697	0.863	0.863	0.182	10.86

LAMINAR FLOW MODEL

TEST #:	C	V _f	Q _p	Q _r	Q _t	Q _m	Q _p /Q _m	P ₁
1	1.89E+11	0.940	0.144	0.694	2.286	0.838	0.172	10.45
2	1.95E+11	0.939	0.140	0.696	2.285	0.836	0.168	10.48
3	2.00E+11	0.939	0.136	0.697	2.285	0.833	0.164	10.51
4	2.04E+11	0.938	0.134	0.698	2.285	0.832	0.162	10.52
5	2.10E+11	0.938	0.131	0.699	2.285	0.830	0.158	10.55
6	2.11E+11	0.938	0.130	0.699	2.285	0.830	0.157	10.56
7	2.14E+11	0.937	0.129	0.700	2.284	0.828	0.155	10.57
8	2.16E+11	0.937	0.128	0.700	2.284	0.828	0.154	10.58
AVG:	2.05E+11	0.938	0.134	0.698	2.285	0.832	0.161	10.53

TURBULENT FLOW MODEL

TEST #:	C	V _f	Q _p	Q _r	Q _t	Q _m	Q _p /Q _m	P ₁
1	1.89E+11	0.850	0.142	0.622	2.277	0.764	0.186	11.42
2	1.95E+11	0.850	0.138	0.624	2.277	0.762	0.181	11.45
3	2.00E+11	0.850	0.135	0.625	2.276	0.760	0.177	11.47
4	2.04E+11	0.849	0.133	0.626	2.276	0.759	0.175	11.49
5	2.10E+11	0.849	0.129	0.628	2.276	0.757	0.171	11.51
6	2.11E+11	0.850	0.129	0.629	2.276	0.757	0.170	11.51
7	2.14E+11	0.849	0.127	0.629	2.276	0.756	0.168	11.53
8	2.16E+11	0.849	0.126	0.629	2.276	0.755	0.167	11.53
AVG:	2.05E+11	0.850	0.132	0.626	2.276	0.759	0.174	11.49

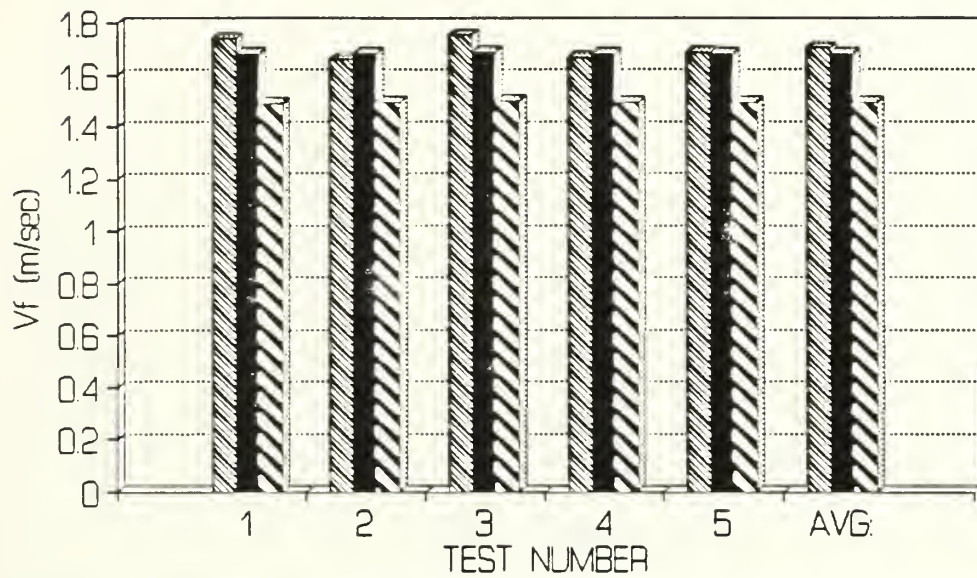
Laminar vs. Turbulent modeling: Both models seem to simulate experimental data reasonably well. This tends to support the idea that the membrane fibers operate in the transition region between laminar and turbulent flows. It should be noted that, by adjusting the K value of the bypass valve in the hydraulic model, one could cause one model to perform better than the other. This is possible because of the turbulent model's increased resistance to fibre flow. This increased resistance tends to increase the cartridge inlet pressure, which can be accurately simulated by increasing the K value of the bypass valve (this in effect "closes" the bypass valve, thereby increasing inlet pressure as well as increasing flow to the membrane).

Discussion: The hydraulic model as written is an effective simulation of hollow fibre membrane flow. The model also contains the flexibility to simulate fouling of the membrane, as well as hollow fibre membranes of varying composition (see appendix A for a description of how the spreadsheet operates). The model's limitation is that it is static in nature; although a dynamic system cannot be simulated directly, it can be configured to simulate incremental changes in time. This is done by making the membrane constant a function of time, solving for the membrane constant for different values of time, then imputing that value into the model and solving the resulting iteration. The membrane constant may be viewed in this regard as the degree to which the membrane is fouled. If, for example, one believes the membrane to foul exponentially, one could make the membrane constant an

exponential function of time, then solve the model for various values of time. This, as we shall see, is the approach used in the section on economic optimization.

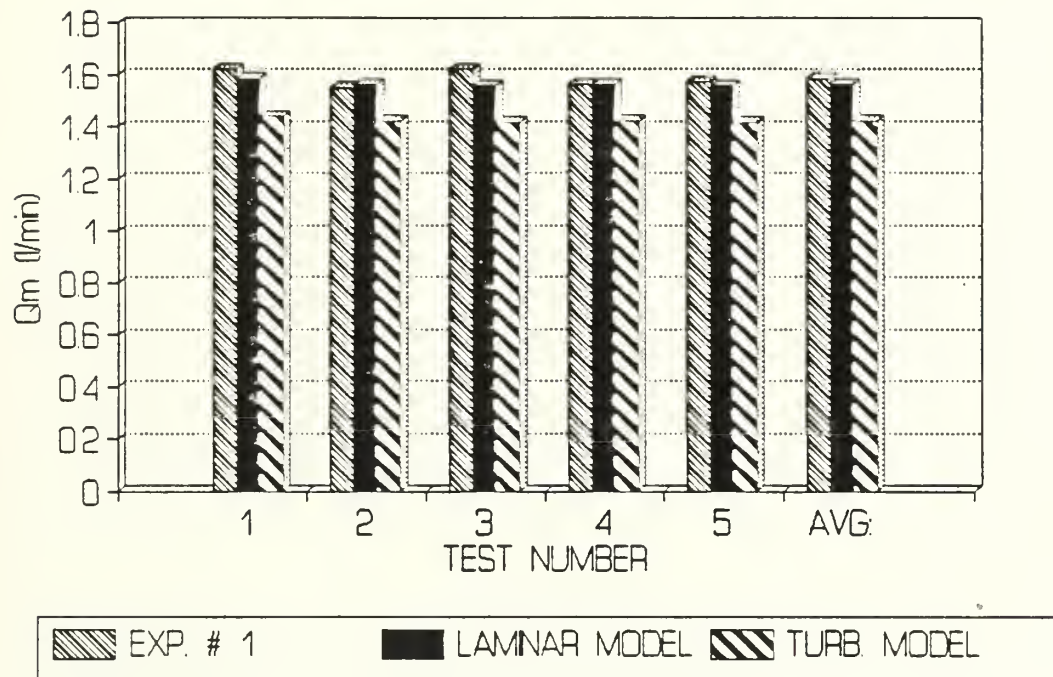
Further research: Several assumptions had to be made in the development of these results; specifically, the use of a pump curve which was not representative of the pumps used in the actual experiments, and a speculation of the values of the bypass valve constant K and bypass flow rate. Further research experiments should be designed to specifically measure bypass flow rate and change in pressure across the bypass valve, as well as permeate and retentate flows and trans-membrane pressure. Further research experiments should also include pumps for which the characteristic pump curve is known. This information is essential in improving the accuracy of the hydraulic model, as well as in providing further insight to the preference of the laminar flow model over the turbulent flow model. Finally, as pointed out in Clark, 1991, an effort should be made to incorporate an irreversible fouling term into the model. This could most easily be done by making the membrane constant an increasing function of permeate flow. The function which the term would take would require considerable research into the fouling mechanisms of the membrane being studied.

COMPARISON OF V_f
FOR EXP. # 1, L.M., AND T.M.

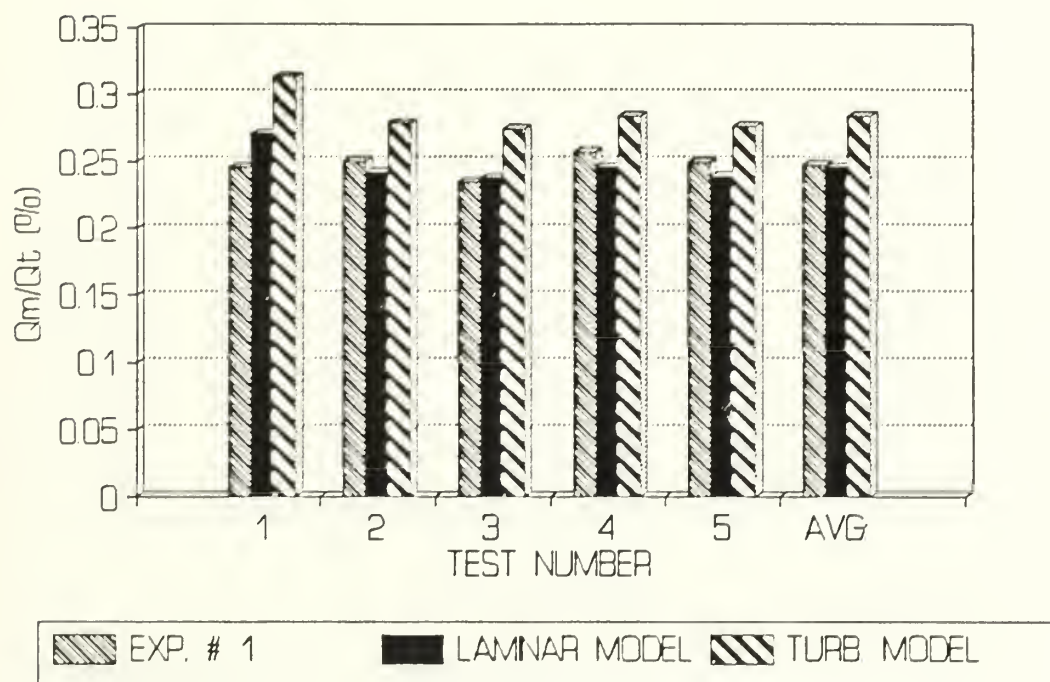


EXP # 1 LAMINAR MODEL TURB. MODEL

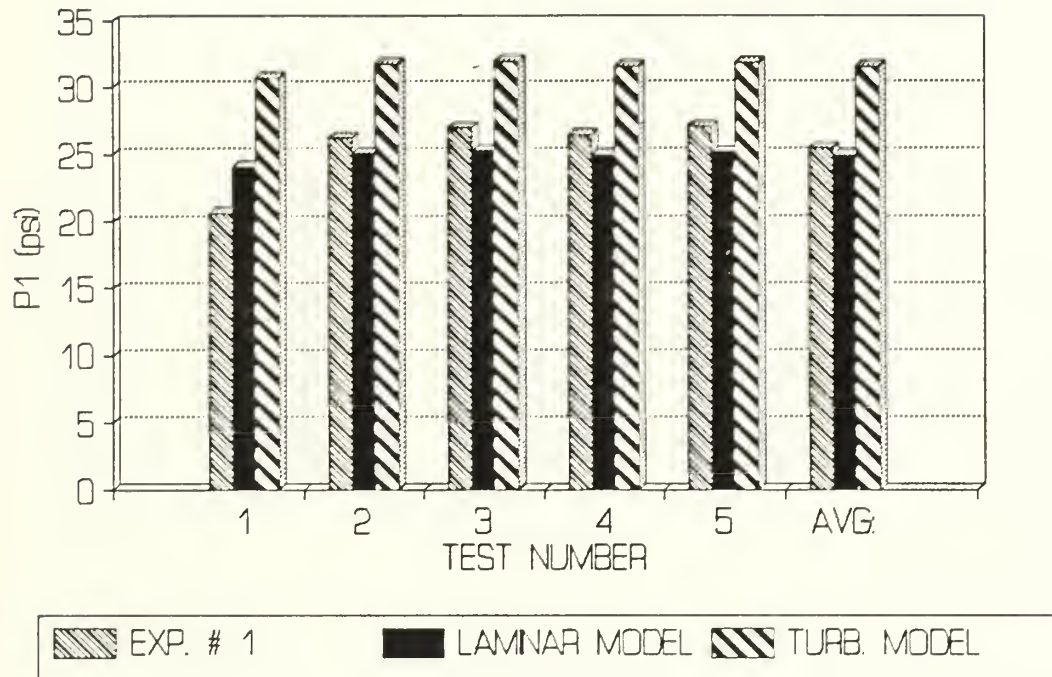
COMPARISON OF Q_m
FOR EXP # 1, L.M., AND T.M.



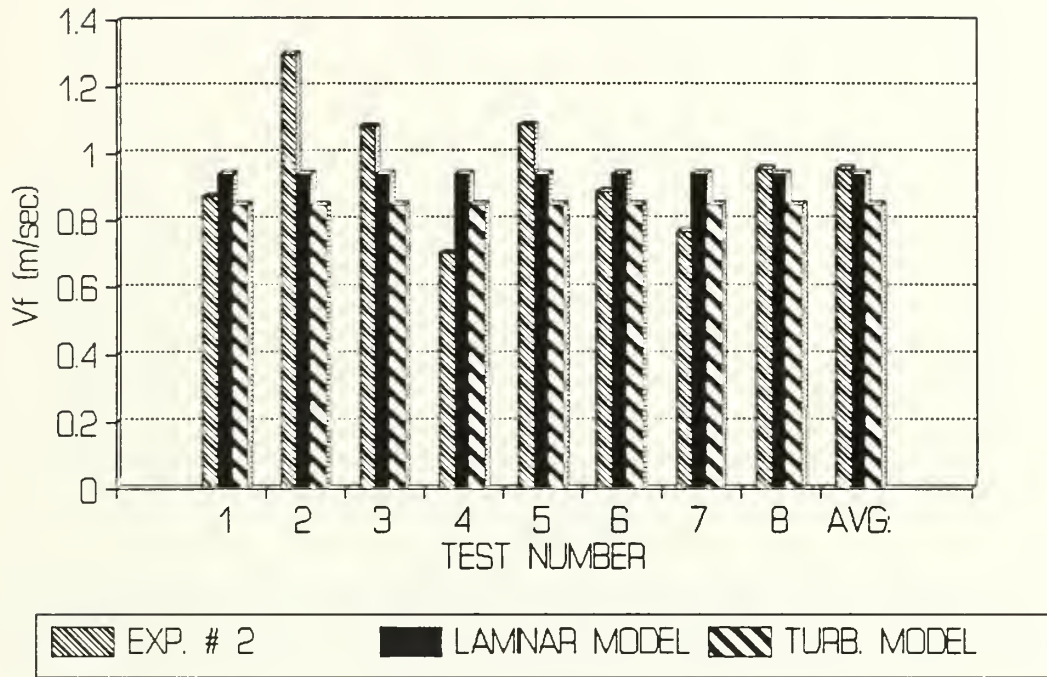
COMPARISON OF Q_p/Q_m
FOR EXP. # 1, L.M., AND T.M.



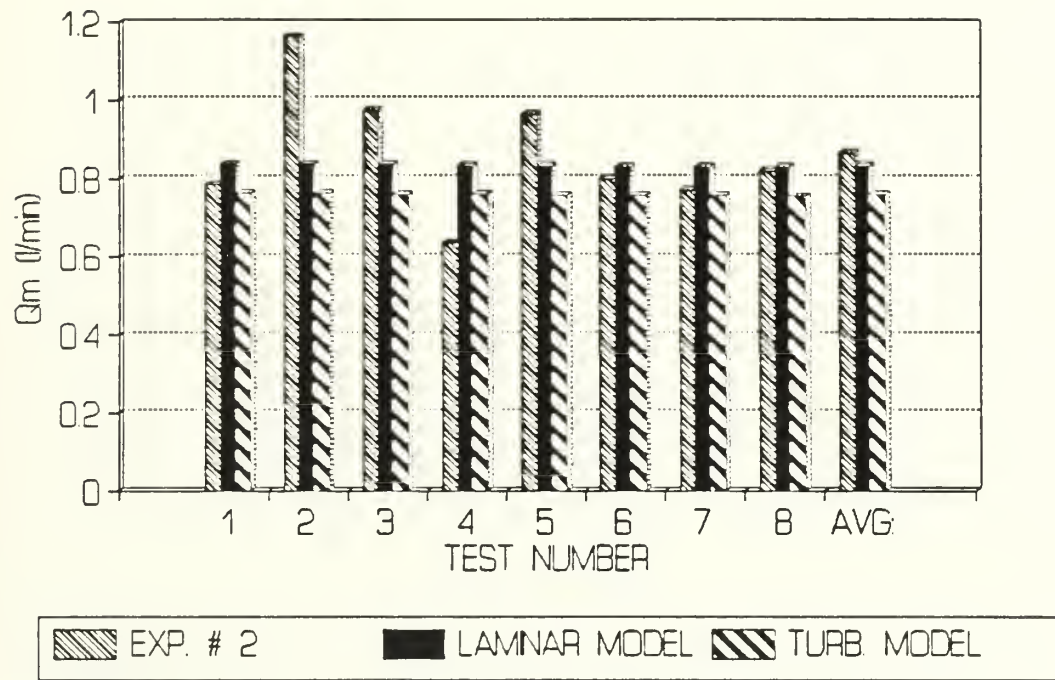
COMPARISON OF P1
FOR EXP. # 1, L.M., AND T.M.



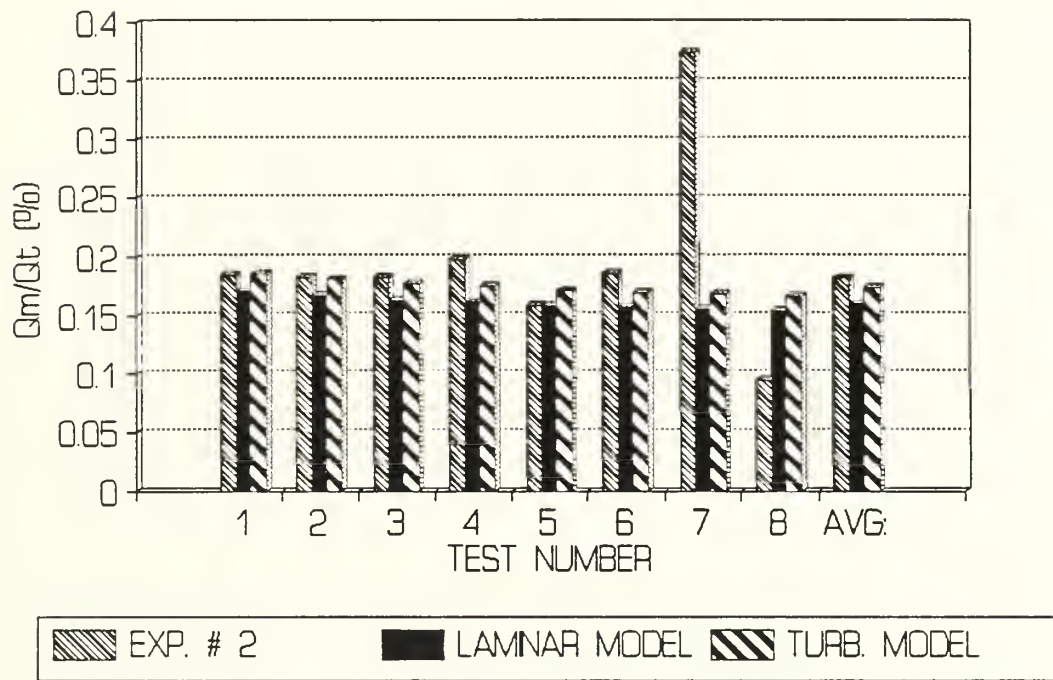
COMPARISON OF V_f
FOR EXP. # 2, L.M., AND T.M.



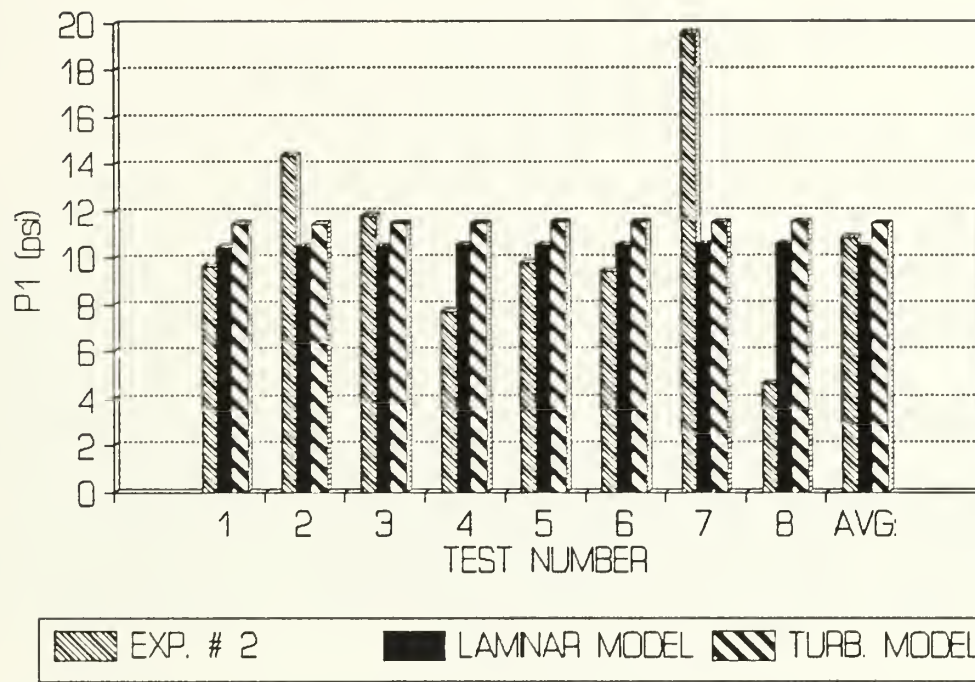
COMPARISON OF Q_m
FOR EXP. # 2, L.M., AND T.M.



COMPARISON OF Q_p/Q_m FOR EXP. # 2, L.M., AND T.M.



COMPARISON OF P1
FOR EXP. # 2, L.M., AND T.M.



ECONOMIC OPTIMIZATION

The cost of UF operations has been discussed in several EPA reports and in other research (Gumerman et al, 1985, Taylor et al, 1989, and Lainé et al, 1991). Gumerman et al (1985) developed capital cost estimates in consideration of treatment plant construction planning. Taylor et al (1989) developed operating cost estimates, to include membrane replacement, for life cycle costs associated with the bench-scale use of spiral wound membranes. In their analysis, Taylor et al used the mass transfer theory model to estimate permeate flux. Lainé et al (1991) related operating costs to UF pump energy costs, without regard for membrane replacement. This report will attempt to optimize operating costs of a UF operation. Amortization of capital costs will not be considered in this analysis.

Because of fouling of the UF membrane during the normal course of operations, it is necessary to backflush the membrane periodically. This backflush serves both to increase the permeate flux and to reduce the pressure head that the pump must work against, thus making the process less expensive. Back flushing, however, requires a source of clean water and, of course, energy. The clean water source is simply the permeate previously generated. We will show that there is an optimal cycle time (one cycle includes one UF period and one backflush period) at which the system should operate; that is to say, a unique cycle time exists for which the volume of permeate produced per kilowatt-hour of energy expended is maximized.

Our intention is to quantify both the permeate produced and energy consumed as functions of time. We may then perform some basic calculus to find the maximum. The energy required of any pump operating at a given flow rate and pressure head is given by

$$\text{Power} = \rho g Q h_p \quad (60)$$

Assuming a pump efficiency of 80%, the energy required to produce flow Q at head h_p is

$$\text{Power} = \frac{\rho g Q h_p}{.8} \quad (61)$$

Substituting the relationship $\Delta P = \rho g h_p$, we get the following:

$$\text{Power} = 1.25 Q \Delta P \quad (62)$$

Applying conversion factors for PSI to N/M^2 and M^3/sec to l/min , the end result is

$$\text{Power} = .1447 Q \Delta P \quad (63)$$

where power is measured in watts. We therefore may find the power delivered to either the UF pump or the backflush pump if we know both the discharge pressure and the flow delivered.

Now that the power relationship has been defined, we need to

express both power and permeate flow as functions of time. Both power and permeate flow have two components; one for UF, and one for backflush. At this point, we need to make some rather bold assumptions about the system hydraulics. Our first assumption is that the UF pump is operating in the high flow, low pressure part of the pump curve, as indicated in figure (13).

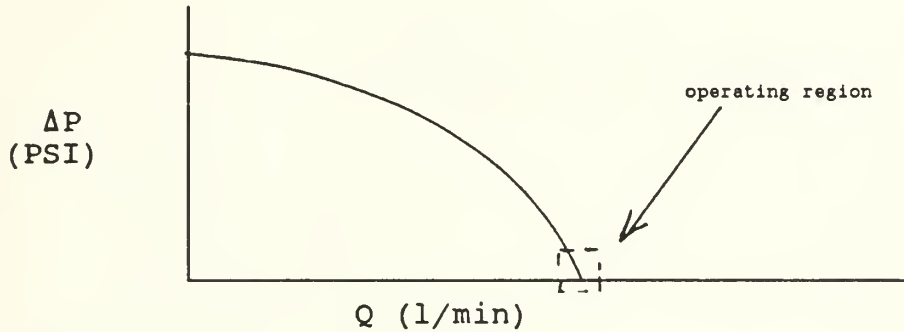


Figure (13)

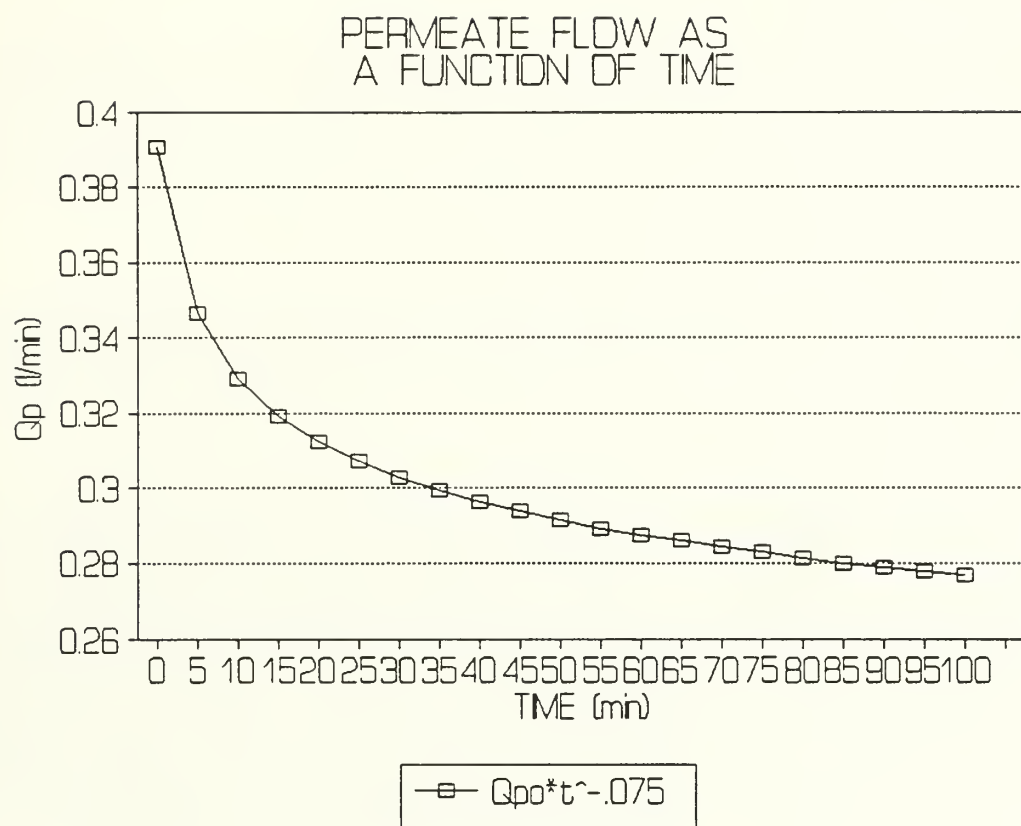
This conforms with the current laboratory set up, and allows us to make the assumption that Q_t , the total UF discharge, is independent of pressure (over the range of values in which we are interested). Although this is an approximation, it is reasonable; the hydraulic model shows that Q_t changes only about 2% over the range of pressures in which we are interested. Our last, and perhaps most inaccurate assumption, is defining how Q_p varies with time. In reality, Q_p is a function of the rate at which the membrane is fouled. Lacking sufficient experimental data, we will use an exponential decay function accepted by many researchers (Cheryan, 1986, p.174):

$$Q_p = Q_{p_0} t^{-.075} \quad (64)$$

Experimental data shows a linear decay of the permeate flux for the first 15 minutes of UF operation (Heneghan, 1991, Adham, 1991), dropping off to about 75% of the original permeate flux. The literature indicates that the decay rate slows considerably after this initial decline (Cheryan, 1986, p.172; Fell, 1990). The coefficient selected in equation (64) approximates these results, and plots as shown in figure (14); it is characterized by a relatively linear decay for the first 15 minutes of the cycle, then exponentially decaying to approximately 75% of the initial value. The curve generated by equation (64) is a "best guess," and should be improved upon by comparison with more extensive experimental data. Integrating equation (64), we get permeate volume as a function of time:

$$V_p(t) = 1.081 Q_{p_0} t^{.925} \quad (65)$$

Now having an expression for permeate flow as a function of time, we can determine permeate flow at any point in time by simple calculation. We can then take these generated values, plug them back into the hydraulic model, and solve for the membrane constant,



C, which corresponds to the desired flow. Each flow will also generate a unique discharge pressure (ΔP), which we can plot against the corresponding times for which the permeate flows were taken. Finally, we can fit a mathematical expression to this curve. For the data in this example, the expression for ΔP as a function of time is:

$$P = P_o + 5.66(1 - t^{-.1}) \quad (66)$$

Figure (15) shows the resulting curve. Note that this curve is based on the data generated by the spreadsheet from equation (64), and should be improved upon by comparison with more extensive experimental data.

Now, substituting equation (66) into the power equation yields

$$Power = .1447 Q (P_o + 5.66(1 - t^{-.1})) \quad (67)$$

Integrating this expression over time results in an equation for the energy delivered to the pump (note unit conversions from watts to kilowatts and from minutes to hours):

$$kWH(t) = 2.41 \times 10^{-6} Q_t [t(P_o + 5.66) - 6.29 t^{.9}] \quad (68)$$

Our goal is to optimize the ratio of Permeate volume to kilowatt-hours consumed. In this regard, we must now account for the power required to drive the backflush pump as well as the permeate volume required for the backflush. We do so as follows: We will make the assumption that the membrane module experiences no irreversible fouling. We will further assume that a one minute backflush will achieve a 100% removal of particulate matter from the membrane (or, 100% recovery of the initial permeate flux). Experimental data for the laboratory set up we have used indicated a backflush pump discharge pressure of about 33 PSI, with a flow rate of .35 l/min. Assuming a constant backflush discharge pressure, we obtain the following results:

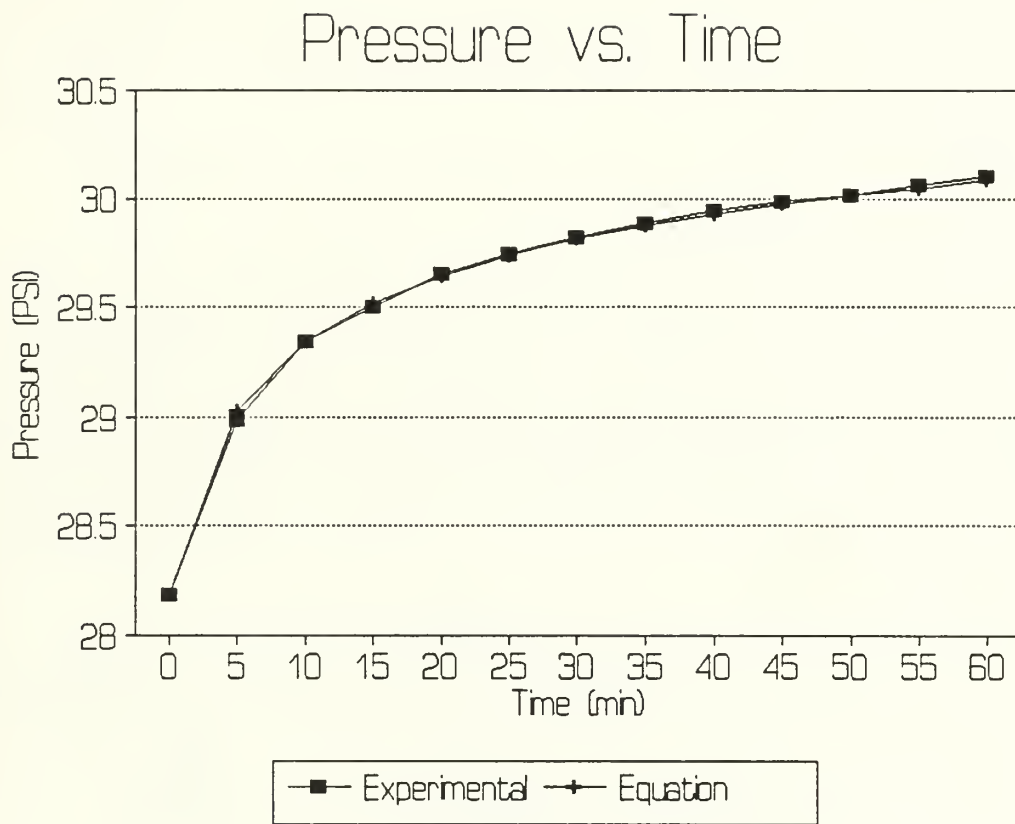
$$kWH = 2.41 \times 10^{-6} Q \Delta P \Delta t = 2.41 \times 10^{-6} (.35) (33) (1)$$

$$kWH = 2.77 \times 10^{-5} kWH \quad (69)$$

$$Vol. = \frac{.35 l}{min} \times 1 min = .35 l$$

It is important to note that we are assuming that a one minute backflush will suffice regardless of the length of the period of UF prior to the backflush. Intuitively, we would suspect that this is not the case, and that the length of the backflush would in actuality be a function of the length of the period of UF. For the moment, we will proceed as planned, and see if our assumption is accurate.

From the above equations we can now predict the permeate volume generated and the energy consumed in one cycle (one cycle = one UF and one backflush period). Combining equations (65), (68), and (69), we get the desired equations for energy and permeate volume:



$$kW \cdot H(t) = 2.41 \times 10^{-6} Q_t [t(P_o + 5.66) - 6.29 t^{.9}] + 2.77 \times 10^{-5} \quad (70)$$

$$V_p(t) = 1.081 Q_{p_o} t^{.925} - .35 \quad (71)$$

We now must determine the time for which the ratio of power to volume is at a maximum. This can be most simply done by dividing equation (71) by equation (70), then take the first derivative with respect to time. Setting the resulting expression to zero and solving for time will provide us with the maximum. The form of the derivative is

$$\frac{d}{dt} \left(\frac{V_p(t)}{kW \cdot H(t)} \right) = \frac{1}{kW \cdot H(t)} \left(\frac{dV_p(t)}{dt} \right) - \frac{V_p(t)}{(kW \cdot H(t))^2} \left(\frac{d kW \cdot H(t)}{dt} \right) \quad (72)$$

Once the derivative is taken, we set the resulting expression equal to zero and solve for time. The mathematics of doing this are somewhat complicated, so instead we will use the spreadsheet and solve by iteration. The results are shown in table (6). A graphical solution is also possible. By dividing equation (71) into equation (70) and solving the resulting expression for various values of time (table 7), we can plot the results as indicated in figure (16), which, as we expect, provides the same conclusion as the calculus solution.

TABLE 6

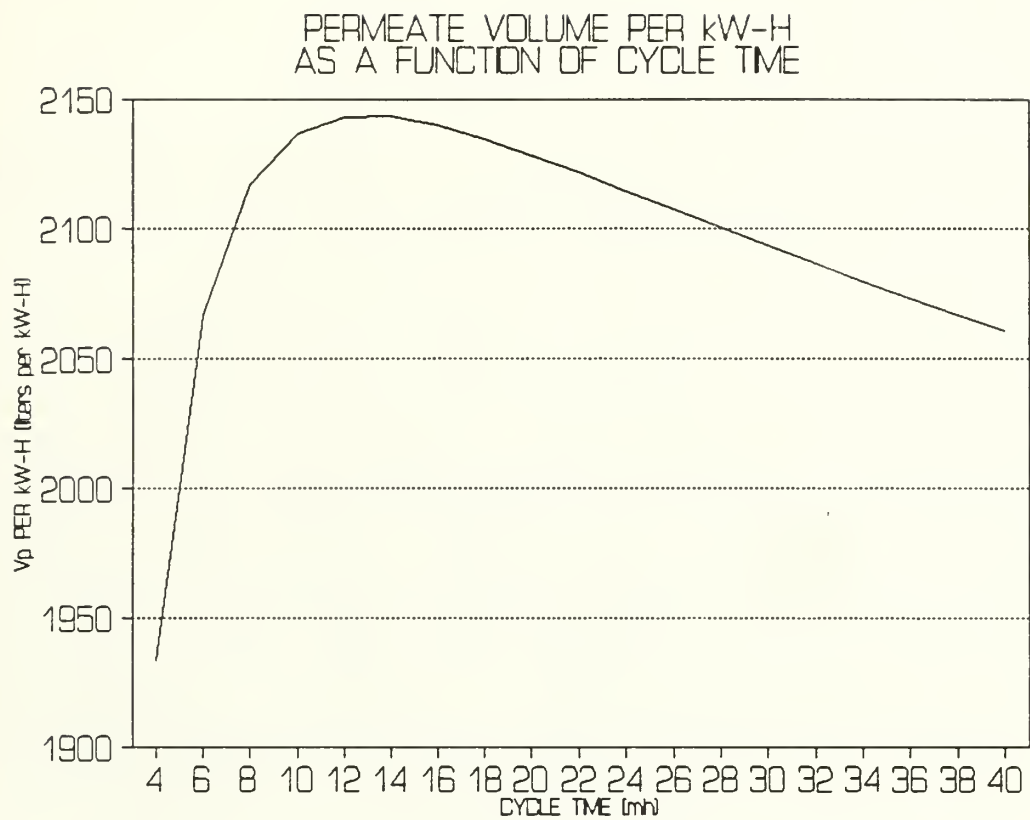
CALCULUS SOLUTION OF MAXIMIZATION OF t FOR EXPONENTIAL DECAY:

Q_p -	0.391	V_p -	4.185
Q_t -	2.119	dV_p/dt -	0.323
ΔP -	28.181	$kW \cdot H$ -	1.95E-03
		$dkW \cdot H/dt$ -	0.00015
t -	13.007	$d/dt(V_p/kW \cdot H)$ -	0.00176

TABLE 7

GRAPHICAL SOLUTION
OPTIMIZATION OF PERMEATE FLOW PER KILOWATT HOUR

t	V_p (min)	$kW \cdot H$ (l/min)	V_p per $kW \cdot H$
4	1.17	6.0708E-04	1933.4
6	1.87	9.0346E-04	2066.7
8	2.54	1.2015E-03	2116.6
10	3.21	1.5007E-03	2136.6
12	3.86	1.8008E-03	2143.2
14	4.50	2.1017E-03	2143.4 ***
16	5.14	2.4033E-03	2140.0
18	5.78	2.7053E-03	2134.8
20	6.40	3.0079E-03	2128.5
22	7.02	3.3109E-03	2121.7



24	7.64	3.6143E-03	2114.6
26	8.26	3.9180E-03	2107.5
28	8.87	4.2221E-03	2100.3
30	9.48	4.5264E-03	2093.3
32	10.08	4.8310E-03	2086.4
34	10.68	5.1359E-03	2079.7
36	11.28	5.4410E-03	2073.1
38	11.88	5.7464E-03	2066.8
40	12.47	6.0519E-03	2060.6

Discussion/further research: The procedure outlined above is an effective procedure to optimize UF operations. Its weakness lies in the assumptions that were required, specifically, the response of the UF system to long-term fouling, and the resulting effect on inlet pressure. Further research should include an experiment which measures permeate flow rate and membrane cartridge inlet pressure over long periods of time in which there is no back flush operations. Attention should also be given to the amount of time required for complete cleaning of the membrane as a function of cycle time (recall, we assumed a one minute back flush would suffice regardless of the length of the UF portion of the cycle). An evaluation of the actual time required for backflush as the UF period becomes longer would be beneficial in further improving the accuracy of the optimization. Finally, the optimization procedure does not account for the size of the UF pump. The pump we used operated in the high flow, low pressure region of the pump operating curve. This suggests that the pump was too large for the system requirements, resulting in considerable bypass flow; as a result, one could make a case for a smaller pump which operates at a lower cost per kilowatt hour, and which has a lower capital cost (an issue not previously discussed, but outside the scope of this report). The trade off in this case is that, although operating costs are initially lower, Q_t would no longer be independent of membrane cartridge inlet pressure. This effect would necessitate a change in the equation for pump power (equation (67)), which must then account for a change in Q_t as a function of time. The corrections could be made with relative ease, and the rest of the procedure followed as indicated.

APPENDIX 1

SPREADSHEET OPERATION

The spreadsheets developed in conjunction with this report were formulated with QUATTRO PRO, version 3.0. In all, three different spreadsheets were written; one for the model in which the bypass valve was not utilized, one for which the bypass line was utilized, and one for the economic optimization. The first two were designed specifically for future manipulation, including evaluation of different pumps, evaluation of the effect of fouling, and for ease of improvement as more experimental data becomes available. The third spreadsheet is little more than a scratch sheet used to solve the economic optimization; because of its relatively simple format, it will not be further discussed. The intention of the rest of this appendix is to familiarize the reader with the use and application of the first two spreadsheets. Details on the use of QUATTRO PRO may be found in the user's guide.

The spreadsheet for the hydraulic model without the bypass line is labeled "MODEL#3.1." The spreadsheet for the model with the bypass line is labeled "MODEL#4.1." The spreadsheets are set up identically, and are operated in the same manner. For explanation purposes, we shall use MODEL#4.1. Figure A-1 shows the layout of the operating portion of the spreadsheet. The spreadsheet is designed to solve for a number of system parameters based on an input value of the membrane constant, C. Once a value of C is entered into the spreadsheet, a non-zero value of "Check P1" will appear in the input. Qt is then iterated upon until "Check P1" is equal to zero. This iteration is most efficiently accomplished by using the /Tools/Solve For command, which can run up to 99 iterations. The iteration must be performed for both the laminar and the turbulent models. Once the iteration is complete, the LAMINAR/TURBULENT FLOW MODEL blocks will indicate the output values of the parameters being evaluated.

In the event that a series of output values are to be evaluated (or graphed), such data may be recorded in the following manner (refer to figure A-2): Use the [ctrl] C command to copy the lower half of the output template onto the upper half as shown in figure A-2. This will replace the old data in the upper half of the template with the cell addresses of the output parameters in figure A-1. As each set of output values is generated, use the /Edit/Values command to replace the cell addresses in the upper half of the template with the actual numbers shown. This procedure in effect preserves the cell address matrix for future use. Note that the values of the membrane constant indicated on the template are for reference purposes only. Because they are not required for any calculations, they may be replaced with the values used to generate the new output. The reader is referred to the QUATTRO PRO user's guide for information concerning the generation of graphs.

The input window in figure A-1 also has a cell for input of the bypass valve constant K. This value may be increased ("closing") or decreased ("opening") as required by the operator. Once experimental data is available to effectively estimate K, it should no longer require adjustment.

The spreadsheet is also designed to allow for changes in the lab configuration or the membrane module used. Figure A-3 shows the input window for the parameters of interest. Such parameters as tubing length and diameter, pump curve constants, viscosity, density, and membrane parameters may be changed.

VALVE K: 1000

LAMINAR FLOW:
Qt: 2.2848
check P1: 0.0001
C = 2.048E+11
TURBULENT FLOW:
Qt: 2.2762
check P1: 0.0003

LAMINAR FLOW MODEL:				TURBULENT FLOW MODEL:			
ADJUST Qt UNTIL CHECK dP = 0				ADJUST Qt UNTIL CHECK dP = 0			
Qp	Qr	Qs	Qt	Qp	Qr	Qs	Qt
0.134	0.698	1.453	2.2848	0.132	0.626	1.518	2.27617
X = 6.324 Y = 12.558 Z = 62.163 F = 4.964 G = 0.552 P1: 10.53 CHECK P1: 0.00				X = 79.327 Y = 12.558 Z = 62.163 F = 4.964 G = 0.552 P1: 11.49 CHECK P1: 0.00			
Az: 0.851 Vf: 0.938 ft: 0.036 At: 0.063 fs: 0.042 Rs: 0.049				Az: 0.851 Vf: 0.115 Vf: 0.850 ft: 0.013 At: 0.023 fs: 0.041 Rs: 0.052			
Qr1 = 0.698 Qr2 = -1.201 Qp = 0.134	Terms			Qr1 = 0.626 Qr2 = -10.526	Check estimation of Qs check P1: -0.005		
Az: Headloss due to height differential Vf: Fiber velocity ft: Tubing friction factor At: Tubing head loss				fs: Bypass valve friction factor Rs: Bypass valve head loss ff: Fiber friction factor			

Figure (A-1)

EVALUATE BOTH MODELS FOR EXPERIMENT #1:

TEST CONDITIONS

TEST #:	C	Vf	Qp	Qr	Qt	Qm	Qp/Qm	P1
1	1.569E+11	1.74	0.398	1.22	1.618	1.618	0.246	206
2	1.874E+11	1.66	0.387	1.16	1.547	1.547	0.250	262
3	1.918E+11	1.75	0.381	1.24	1.621	1.621	0.235	27
4	1.821E+11	1.67	0.402	1.16	1.562	1.562	0.257	26.5
5	1.905E+11	1.69	0.393	1.18	1.573	1.573	0.250	27.1
AVG:	1.818E+11	1.70	0.392	1.192	1.584	1.584	0.247	25.48

LAMINAR FLOW MODEL

TEST #:	C	Vf	Qp	Qr	Qt	Qm	Qp/Qm	P1
1	1.569E+11	1.680	0.428	1.155	2.152	1.584	0.271	24.073
2	1.874E+11	1.684	0.376	1.185	2.142	1.561	0.241	25.114
3	1.918E+11	1.685	0.369	1.189	2.140	1.558	0.237	25.264
4	1.821E+11	1.684	0.384	1.180	2.143	1.564	0.246	24.956
5	1.905E+11	1.684	0.372	1.187	2.141	1.559	0.239	25.205
AVG:	1.818E+11	1.684	0.384	1.180	2.143	1.564	0.246	24.956

TURBULENT FLOW MODEL

TEST #:	C	Vf	Qp	Qr	Qt	Qm	Qp/Qm	P1
1	1.569E+11	1.490	0.451	0.989	2.082	1.440	0.313	30.746
2	1.874E+11	1.497	0.396	1.022	2.071	1.418	0.279	31.783
3	1.918E+11	1.498	0.388	1.027	2.070	1.415	0.274	31.929
4	1.821E+11	1.496	0.404	1.017	2.073	1.421	0.284	31.627
5	1.905E+11	1.497	0.391	1.025	2.070	1.416	0.276	31.874
AVG:	1.818E+11	1.496	0.404	1.017	2.073	1.421	0.284	31.627

STORE TEST RESULTS MATRIX

LAMINAR FLOW MODEL

TEST #:	C	Vf	Qp	Qr	Qt	Qm	Qp/Qm	P1
1	1.569E+11	+\$Q\$29	+\$M\$26	+\$N\$26	+\$P\$12	+\$Q\$26	+\$R\$26	+\$N\$34
2	1.874E+11	+\$Q\$29	+\$M\$26	+\$N\$26	+\$P\$12	+\$Q\$26	+\$R\$26	+\$N\$34
3	1.918E+11	+\$Q\$29	+\$M\$26	+\$N\$26	+\$P\$12	+\$Q\$26	+\$R\$26	+\$N\$34
4	1.821E+11	+\$Q\$29	+\$M\$26	+\$N\$26	+\$P\$12	+\$Q\$26	+\$R\$26	+\$N\$34
5	1.905E+11	+\$Q\$29	+\$M\$26	+\$N\$26	+\$P\$12	+\$Q\$26	+\$R\$26	+\$N\$34
AVG:	1.818E+11	+\$Q\$29	+\$M\$26	+\$N\$26	+\$P\$12	+\$Q\$26	+\$R\$26	+\$N\$34

TURBULENT FLOW MODEL

TEST #:	C	Vf	Qp	Qr	Qt	Qm	Qp/Qm	dP
1	1.569E+11	+\$W\$3	+\$S\$26	+\$T\$26	+\$P\$18	+\$W\$2	+\$X\$26	+\$T\$34
2	1.874E+11	+\$W\$3	+\$S\$26	+\$T\$26	+\$P\$18	+\$W\$2	+\$X\$26	+\$T\$34
3	1.918E+11	+\$W\$3	+\$S\$26	+\$T\$26	+\$P\$18	+\$W\$2	+\$X\$26	+\$T\$34
4	1.821E+11	+\$W\$3	+\$S\$26	+\$T\$26	+\$P\$18	+\$W\$2	+\$X\$26	+\$T\$34
5	1.905E+11	+\$W\$3	+\$S\$26	+\$T\$26	+\$P\$18	+\$W\$2	+\$X\$26	+\$T\$34
AVG:	1.818E+11	+\$W\$3	+\$S\$26	+\$T\$26	+\$P\$18	+\$W\$2	+\$X\$26	+\$T\$34

SYSTEM PARAMETERS:
Q's ARE N l/min, dP IS N psig, AREAS ARE N m²
LENGTHS AND DIAMETERS ARE N m

PARAMETERS:	6895
	60000
PUMP CURVE: A =	A = -36.943
B =	B = 61.66335
C =	C = 63.40662
MEMBRANE CONSTANT =	C = 2.05E+11
VISCOSITY =	u = 9.418E-04
CARTRIDGE SURFACE AREA =	Acart = 0.06
FIBRE LENGTH =	Lf = 1.02
FIBRE DIAMETER =	df = 9.30E-04
FIBRE CROSS SECTION =	af = 6.793E-07
FIBRE ROUGHNESS:	ef = 7.64E-05
DENSITY OF INFLUENT =	p = 997.4
BACK PRESSURE VALVE CONST. =	K = 2530
CROSS SECTION OF RETENTATE T	Abp = 6.362E-05
CROSS SECTION OF NF. TUBE:	At = 6.362E-05
LENGTH OF NF. TUBING:	Lt = 0.6
NF. TUBE DIAMETER:	dt = 0.009
dZ FROM PUMP TO MEMBRANE:	dZ = 0.6
NF. TUBE ROUGHNESS:	e = 1.5E-06
BYPASS VALVE K:	K = 1000
BYPASS TUBE LENGTH:	Ls = 1
CROSS SECTION OF BYPASS TUBING =	6.362E-05
DIAMETER OF BYPASS TUBE:	ds = 0.009

REFERENCES:

Adham, S. S.: Ultrafiltration of Groundwater with Powdered Activated Carbon Pre-treatment for Organic Removal. Ph.D. Thesis, University of Illinois, Department of Civil Engineering. (ongoing research to be completed in 1993).

Cheryan, Munir: Ultrafiltration Handbook. Lancaster, Pa.; Technomic Publishing Company, 1986.

Clark, Mark M.: A Resistance Model for Predicting Flux Decline in Pilot Scale Hollow Fiber Ultrafiltration. Unpublished memorandum; University of Illinois, Department of Civil Engineering, April 6, 1991.

Fell, C. J. D., K. J. Kim, V. Chen, D. E. Wileg, and A. G. Fane: Factors Determining Flux and Rejection of Ultrafiltration Membranes. Center for Membrane and Separation Technology, University of New South Wales, Kensington, N.S.W., 2073 (Australia). Chemical Engineering Processes, 27, 1990; pp. 165-173.

Gumerman, Robert C. Bruce E. Burris, and Sigurd P. Hansen, Culp/Wesner/Culp Consulting Engineers: Estimation of Small System Water Treatment Costs. Contract # 68-03-3093, Municipal Environmental Research Laboratory., Office of Research and Development, U. S. Environmental Protection Agency, Cincinnati, Ohio 45268. 1985.

Heneghan, Karen: Ultrafiltration with PAC and Alum Pre-treatment: A Preliminary Pilot Scale Investigation. Master's Thesis, University of Illinois, Department of Civil Engineering. (ongoing research, to be completed in 1991).

Lainé, Jean-Michel, James P. Hagstrom, Mark M. Clark, and Joël Mallevalle: Effects of Ultrafiltration Membrane Composition. Journal of the AWWA, November, 1989, pp.61-68.

Lainé, Jean-Michel, Mark M. Clark, and Joël Mallevalle: Ultrafiltration of Lake Water: Effect of Pretreatment on the partitioning of Organics, THMFP, and Flux. Journal of the AWWA, December, 1990, pp.82-85.

Lainé, Jean-Michel, Joseph G. Jacangelo, Nancy L. Patania; James M. Montgomery, Consulting Engineers, Inc., Booe, Wayne, Boise Water Corporation, and Mallevalle, Joël, Lyonnaise des Eaux-Dumez: Evaluation of Ultrafiltration Membrane Fouling and Parameters for its Control. AWWA Membrane Technology and Its Applications in the Water Industry; Orlando, Fla. March 10-13, 1991.

Taylor, J. S., L. A. Mulford, W. M. Barrett, S. J. Duranceau, D. K. Smith: Cost Performance of Membranes for Organic Control in Small Systems: Flagler Beach and Punta Gorda, Florida. Cooperative Agreement No. CR 813199; Drinking Water Research Division, Risk Reduction Laboratory, Cincinnati, Ohio 45268; August 9, 1989.

White, Frank M.: Fluid Mechanics. New York; McGraw-Hill, Inc.; 1986. 2nd ed.

Thesis
02442
c.1

Odderstol
Hydraulic modeling and
economic optimization
of hollow fiber mem-
branes.

Tlesis

02442
c.1

Odderstol
Hydraulic modeling and
economic optimization
of hollow fiber mem-
branes.

DUDLEY KNOX LIBRARY



3 2768 00016481 8